Distances between the Paclitaxel, Colchicine, and Exchangeable GTP Binding Sites on Tubulin†

Yi Han,‡ Henryk Malak,§ A. G. Chaudhary,|| M. D. Chordia,|| David G. I. Kingston,|| and Susan Bane*,‡

Department of Chemistry, State University of New York at Binghamton, Binghamton, New York 13902-6016, Center for Fluorescence Spectroscopy, University of Maryland School of Medicine, Baltimore, Maryland 21201, and Department of Chemistry, Virginia Polytechnic Institute and State University, Blacksburg, Virginia 24061-0212

Received August 11, 1997; Revised Manuscript Received November 25, 1997

ABSTRACT: Distances between the paclitaxel, colchicine, and exchangeable GTP binding sites on tubulin polymers have been probed using fluorescence spectroscopy. Techniques for measuring fluorescence resonance energy transfer (FRET) between fluorescent or chromophoric ligands for each binding site were employed. 2-Debenzoyl-2-(*m*-aminobenzoyl)paclitaxel (2-AB-PT) was the fluorophore ligand for the paclitaxel binding site; thiocolchicine, allocolchicine, and MDL 27048 were probes for the colchicine site, and 2′(or 3′)-*O*-(trinitrophenyl)guanosine 5′-triphosphate (TNP-GTP) was the fluorophore ligand for the exchangeable GTP site. The distance between the colchicine and paclitaxel binding sites was determined with two different acceptor ligands in the colchicine site. An average distance distribution of 17 Å was found in both cases. Energy transfer between 2-AB-PT bound to the paclitaxel site and TNP-GTP (acceptor) bound to the exchangeable GTP site was observed in the polymer. The average distance distribution between the fluorophores was 16.0 Å, but the half-width of the distribution was large (17.9 Å), which indicates that energy transfer between more than one donor−acceptor pair occurred in the system. One interpretation of this result is that 2-AB-PT serves as an energy transfer donor for two GTP sites, one contained on the same subunit and one on an adjacent protofilament. No FRET was observed between ligands bound to the colchicine and exchangeable GTP sites, indicating that the result of colchicine binding on the GTP region of β-tubulin is a long range, allosteric effect. The results from these experiments are interpreted in terms of known structural features of microtubules.

Microtubules are an integral part of the cytoskeleton of all eukaryotic cells. These structures participate in a vast number of cellular functions, including mitosis, morphogenesis, intracellular transport, and secretion (*1*). The cylinder lattice of the microtubule is composed entirely of the protein tubulin, which is a highly conserved heterodimeric protein. Microtubules are formed by the reversible assembly of soluble tubulin into polymers and possess in vivo additional proteins such as microtubule-associated proteins and motor proteins on the surface of the lattice. Other proteins are not required for microtubule assembly in vitro; normal microtubules can be produced from purified tubulin under certain conditions (*2*).

The pathway from soluble tubulin to the functional microtubule polymer is remarkably sensitive to endogenous and exogenous effectors (*3*). As a result, tubulin has been an important target for chemotherapy, with particular success as a receptor for antineoplastic agents. Drugs such as paclitaxel (Taxol), vincristine, and estramustine are widely used in cancer chemotherapy, and new tubulin-active drugs, such as the cryptophycins, have progressed to clinical testing (*4*−*6*). It appears that all these drugs interact with tubulin at or in the vicinity of only three binding sites, known as the colchicine, *Vinca*, and paclitaxel binding sites (*7*). Drug binding to the each site produces effects on gross polymer morphology that tend to be characteristic of the binding site involved. For example, most ligands that bind to the colchicine site on tubulin associate with the protein prior to its polymerization and subsequently inhibit assembly (*8*), while ligands that bind to the paclitaxel site on tubulin stimulate assembly and bind preferentially to tubulin polymers (*9*, *10*). Drug binding to the *Vinca* site inhibits tubulin assembly at low concentrations, but at higher concentrations induces tubulin self-association into nonmicrotubule structures and into paracrystals (*11*).

The drug binding sites also appear to be linked to some degree. Paclitaxel will promote tubulin assembly into microtubules in the presence of calcium and in absence of GTP,[1] and the resulting polymers are cold-stable. If colchicine is bound to tubulin prior to treatment with paclitaxel,

† This work was supported in part by National Institutes of Health Grants CA55131 and CA48974 (to D.G.I.K.) and National Science Foundation Grant MCB9406424 (to S.B.).

* To whom correspondence should be addressed.
‡ State University of New York at Binghamton.
§ University of Maryland School of Medicine.
|| Virginia Polytechnic Institute and State University.

[1] Abbreviations: 2-AB-PT, 2-debenzoyl-2-(*m*-aminobenzoyl)paclitaxel; DMSO, dimethyl sulfoxide; MDL 27048, *trans*-1-(2,5-dimethoxyphenyl)-3-[4-(dimethylamino)phenyl]-2-methyl-2-propen-1-one; EGTA, ethylene glycol bis(β-aminoethyl ether)-*N*,*N*,*N*′,*N*′-tetraacetic acid; GTP, guanosine 5′-triphosphate; PIPES, piperazine-*N*,*N*′-bis(2-ethanesulfonic acid); PME1 buffer, 50 mM PIPES, 0.5 mM $MgSO_4$, and 1 mM EGTA at pH 6.9; PME2 buffer, 100 mM PIPES, 1 mM $MgSO_4$, and 2 mM EGTA at pH 6.9; PMEG buffer, 100 mM PIPES, 1 mM $MgSO_4$, 2 mM EGTA, and 0.1 mM GTP at pH 6.9.

S0006-2960(97)01976-4 CCC: $15.00
Published on Web 04/28/1998

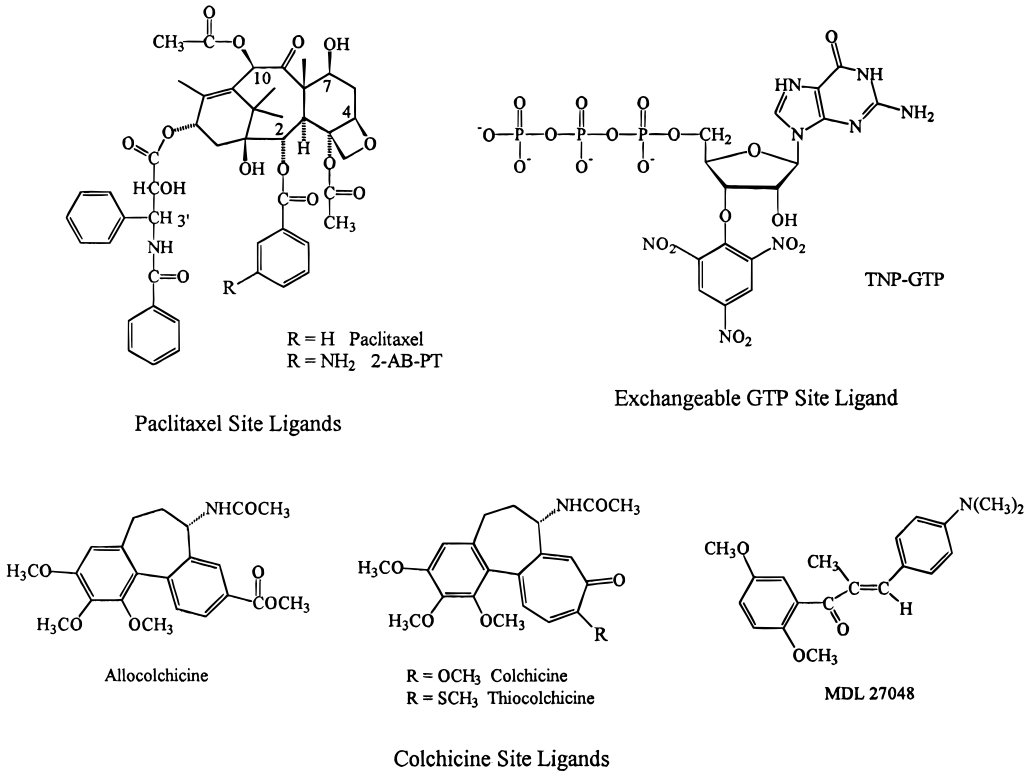

FIGURE 1: Structures of ligands.

however, sheets of protofilaments, spirals, and amorphous aggregates rather than microtubules are formed. Assembly of tubulin−colchicine into these polymers requires exogenous GTP and is reversed with cooling (*12*). In addition, ligand binding to the colchicine site generally activates a weak GTPase activity in tubulin, while binding of the *Vinca* alkaloids to tubulin inhibits this GTPase activity (*13*). Paclitaxel induces additional GTPase activity in the tubulin−colchicine complex (*14*).

It is clear that tubulin binding by each class of drug affects the conformation of the protein in measurable but poorly understood ways (*15*). It is likely that these ligand-induced conformational states of tubulin are responsible for the aberrant assembly properties of the protein. Although it is possible to measure what is happening to the protein when the drugs bind, there is currently no information about how the drugs affect the protein conformation and why drug binding to the three sites results in such different macromolecular morphologies. For example, does paclitaxel binding remove the GTP requirement for tubulin assembly because it induces a GTP-like conformation in the protein? And if so, is the effect mediated by a subtle, localized conformational change or is it the result of a long range, allosteric effect that involves a substantial region of the protein?

A detailed three-dimensional structure of tubulin would be most helpful in beginning to address such questions. Currently, the structure of tubulin in zinc-induced tubulin sheets has been resolved to 4 Å (*16*), which is not a high enough resolution to identify the individual amino acids in the protein. Moreover, a three-dimensional structure would need to contain information about the location of the drug and small molecule binding sites on the protein. Solving multiple structures of a protein the size of tubulin, if appropriate samples could be prepared, would require colossal effort and resources. Data from affinity and photoaffinity labeling experiments might be of help in locating ligand binding sites on an eventual three-dimensional structure. Photoaffinity labeling, however, rarely identifies a single amino acid or even a single peptide in the primary structure of a protein (*17*).

A technique for evaluating the spatial relationships between ligand binding sites on tubulin that provides dependable accuracy and requires moderate resources is measurement of fluorescence resonance energy transfer (FRET). FRET has been described as a "spectroscopic ruler", capable of measuring distances of up to 70 Å between fluorophores (*18*). Time-resolved measurements of FRET, now more generally accessible with commercial instrumentation, can provide an abundance of additional information about the spatial relationships between fluorophores in biological systems (*19*). FRET measurements have been performed on tubulin to determine the distance between the colchicine and Ruthenium Red binding sites on the protein (40−45 Å; *20*) and to estimate the minimum distances between other ligand binding sites on tubulin (*20, 21*). In this work, we use FRET to examine the distances between the colchicine, paclitaxel, and exchangeable GTP binding sites on tubulin using fluorescent ligands (Figure 1). On the basis of these FRET results and recent information regarding tubulin topology, a possible arrangement of these binding sites on tubulin and the microtubule is proposed.

EXPERIMENTAL PROCEDURES

Materials. 2-Debenzoyl-2-(*m*-aminobenzoyl)paclitaxel (2-AB-PT) was prepared from paclitaxel by semisynthesis as described by Han et al. (*22*). Allocolchicine was prepared from colchicine as described by Hastie (*23*). 2′(or 3′)-*O*-(trinitrophenyl)guanosine 5′-triphosphate, trisodium salt (TNP-GTP) was purchased from Molecular Probes, Inc. *trans*-1-

(2,5-Dimethoxyphenyl)-3-[4-(dimethylamino)phenyl]-2-methyl-2-propen-1-one (MDL 27048) was a kind gift from V. Peyrot. Thiocolchicine was prepared by semisynthesis from colchicine (*24*).

PIPES and EGTA were obtained from Sigma. Spectrograde solvents were used in absorption and fluorescence spectroscopy.

Tubulin Purification and Protein Determination. Bovine brain tubulin, free of microtubule-associated proteins, was prepared by two cycles of assembly−disassembly followed by phosphocellulose chromatography (*25*) and stored in liquid nitrogen. Prior to use, the frozen pellets were gently thawed, centrifuged at 5000*g* for 10 min at 4 °C, and then desalted into the desired buffer on 1 mL Sephadex G-50 columns according to the method of Penefsky (*26*). Tubulin concentrations were determined spectrophotometrically in PME buffer using an ϵ_{278nm} of 1.23 (mL/mg) cm^{-1} (*27*). The concentrations of 2-AB-PT, thiocolchicine, and MDL 27048 were also determined spectrophotometrically using the following extinction coefficients: 2-AB-PT, $\epsilon_{320nm} = 2.85 \times 10^3$ M^{-1} cm^{-1} in PME buffer containing 10% DMSO; thiocolchicine, $\epsilon_{380nm} = 1.7 \times 10^4$ M^{-1} cm^{-1} in PME buffer (*28*); and MDL 27048, $\epsilon_{398nm} = 2.1 \times 10^4$ M^{-1} cm^{-1} in aqueous buffer containing 4% DMSO (*29*).

Preparation and Characterization of Tubulin−TNP-GTP. Replacement of E-Site GTP with GDP. Tubulin−GDP was prepared using a modified procedure from Seckler et al. (*30*). First, tubulin (40 μM) was incubated with excess GDP (5 mM) on ice for 20 min in PME2 buffer. Then, unbound GTP and GDP in the protein solution were removed by rapid gel filtration of Penefsky (*26*), resulting in tubulin−GDP.

Characterization of Tubulin−GDP. Tubulin−GDP was evaluated for nucleotide contents by extracting nucleotides and the subsequent quantitative determination of GTP/GDP by HPLC. Nucleotides were extracted from tubulin by the method of Seckler et al. (*30*). Ice cold $HClO_4$ was added to a final concentration 0.5 M into the tubulin−GDP solution prepared as described above, and the mixture was incubated on ice for 10 min to precipitate the protein. The solution was centrifuged to pellet the denatured protein. The supernatant was carefully removed, titrated with 3 M KOH to neutralize the extra $HClO_4$, and buffered with $^1/_6$ volume of 1 M K_2HPO_4/acetic acid buffer (pH 6.9). The resultant solution was incubated on ice for 10 min at 4 °C and then centrifuged for 10 min in an Eppendorf microcentrifuge at 4 °C to pellet the remaining protein. The supernatant was filtered through a Millipore filer (type HV, 0.45 cm) before HPLC analysis to remove any particulates. HPLC was performed on a Waters μBondapak reversed phase C-18 column (3.9 × 300 mm). The mobile phase was 150 mM KH_2PO_4/KOH and 1 mM TBA (pH 5.9). The nucleotides were detected at 253 nm. The system was calibrated with standard samples of GTP and GDP.

Preparation of Tubulin−TNP-GTP. Tubulin−GDP (40 μM) prepared as described above was incubated with TNP-GTP (800 μM) for 2 h on ice. Unbound TNP-GTP was removed by rapid gel filtration (*26*). Additional TNP-GTP was added to the solution to achieve a final concentration of 50 μM, and the solution was incubated on ice for 3 h. The resultant tubulin−TNP-GTP was stored in liquid nitrogen. Prior to use, tubulin−TNP-GTP was thawed and analyzed by absorption spectroscopy to determine the amount of TNP-GTP bound to tubulin dimer using an ϵ_{408nm} of 2.3 × 10^4 M^{-1} cm^{-1} for TNP-GTP bound to tubulin. This extinction coefficient was determined to be the same as that of unbound TNP-GTP in aqueous buffer (Y. Han and S. Bane, unpublished data).

Preparation of Tubulin−Ligand Samples for FRET. Preparation of Tubulin−TNP-GTP−2-AB-PT. Tubulin−TNP-GTP was prepared as described above. Tubulin−TNP-GTP−2-AB-PT for the fluorescence studies was prepared by incubating tubulin−TNP-GTP (5 μM) with 2-AB-PT (2.5 μM) at 37 °C for 30 min in PME2 buffer.

Preparation of Tubulin−TNP-GTP−Allocolchicine. Tubulin−TNP-GTP was prepared as described above. Tubulin−TNP-GTP−allocolchicine was prepared by incubating tubulin−TNP-GTP (5 μM) with allocolchicine (5 μM) at 37 °C for 2 h. The concentration of allocolchicine was chosen to avoid inner filter effects.

Preparation of Tubulin−Thiocolchicine and Tubulin−Thiocolchicine−2-AB-PT. Tubulin (20 μM) was incubated with a 10-fold molar excess of thiocolchicine at 37 °C for 30 min in PME1 buffer. Excess thiocolchicine was removed by rapid gel filtration (*26*). Tubulin−thiocolchicine−2-AB-PT was prepared by incubating 5 μM tubulin−thiocolchicine with 5 μM 2-AB-PT at 20 °C for 20 min.

Preparation of Tubulin−MDL 27048 and Tubulin−MDL 27048−2-AB-PT. Tubulin−MDL 27048 was prepared by incubating tubulin (5 μM) with MDL 27048 (5 μM) in PME1 buffer at 20 °C for 20 min. Tubulin−MDL 27048−2-AB-PT was prepared by incubating 5 μM tubulin with 5 μM MDL 27048 and 5 μM 2-AB-PT at 20 °C for 20 min.

Absorption Spectroscopy. Absorption spectra were measured on a Hewlett-Packard model 8451A diode array spectrometer at ambient temperature. The digitized data were transferred to an IBM-AT computer interfaced with the instrument.

Electron Microscopy. Electron micrographs were obtained using a Hitachi 7000 TEM instrument. Samples were prepared on 200 mesh hydrophilic carbon-coated grids and were stained with uranyl acetate.

Steady-State Fluorescence Spectroscopy. Excitation and emission spectra were recorded on an SLM 48000s spectrofluorometer. The appropriate temperature was maintained with a circulating ethylene glycol−water bath. A 2 × 10 mm quartz fluorescence cell was used and oriented such that the excitation beam passed through the smaller path. Emission spectra were uncorrected. Appropriate background spectra were recorded and digitally subtracted from all presented spectra.

Frequency-Domain Fluorescence Spectroscopy. Frequency-domain measurements were performed on an instrument working up to 5 GHz described previously (*30*). The modulated excitation was provided by the harmonic content of a laser pulse train with a repetition rate of 4 MHz and a pulse width of 7 ps, from a cavity-dumped pyridine dye laser. The dye laser was pumped with a mode-locked argon ion laser (Coherent). The dye laser output was frequency doubled to 335−365 nm with a frequency doubler (Spectra Physics, model C-390). The emitted light was observed with a microchannel photomultiplier. The emission was observed through a 400 nm cutoff emission filter. The measurements were performed under the magic angle polarizer orientations.

Determination of Forster Distances between the Donor and Acceptor Sites. The Forster distance between the donor and the acceptor sites (R_0), which is the distance at which the energy transfer efficiency is 50%, was determined from the following equation:

$$R_0 = (9.79 \times 10^3)(\kappa^2 n^{-4} \phi_d J)^{1/6}$$

where J is the spectral overlap integral between the donor fluorescence emission spectrum and the acceptor absorption spectrum, κ^2 is the factor describing the relative orientation between the transition dipole of donor and that of the acceptor, ϕ_d is the quantum yield of the donor in the absence of the acceptor, and n is the refractive index of the medium (see, for example, ref *19*).

The spectral overlap integral, J, was calculated by numerical integration; κ^2 was assumed equal to $^2/_3$, which is the value for donors and acceptors rotating randomly before energy transfer occurs (*31*). The quantum yields of 2-ABPT bound to microtubules and allocolchicine bound to tubulin were previously determined to be 0.15 (*22*) and 0.29 (*23*), respectively. The refractive index of water (1.33) was used for the calculation.

Determination of the Distance Distribution between Donor and Acceptor Sites. Distance distributions between fluorescence donors and acceptors can be recovered from the intensity decay kinetics of the donors (*30, 32*). The intensity decay of the donor in the absence of the acceptor can be described by

$$I_D(t) = I_D{}^0 \sum_i \alpha_{D_i} \exp(-t/\tau_{D_i}) \quad (1)$$

where $I_D{}^0$ is the intensity of the donor emission at time 0 and α_{D_i} are the relative initial intensities (at $t = 0$) of the particular exponential components that are characterized by the decay times τ_{D_i}. In the case of FRET, the energy transfer rate depends on distance and is given by

$$k_{DA_i}(r) = \frac{1}{\tau_{D_i}}\left(\frac{R_0}{r}\right)^6 \quad (2)$$

where r is the distance between donor and acceptor and R_0 is the distance at which the energy efficiency is 50%, which can be determined by using eq 1.

The probability function $P(r)$, which describes the distribution of donor−acceptor distances, is parameterized on the basis of a Gaussian model:

$$P(r) = \frac{1}{Z}\exp\left[-\frac{1}{2}\left(\frac{r - R_{av}}{\sigma}\right)^2\right] \text{ for } r_{min} \le r \le r_{max}, \text{ or}$$
$$P(r) = 0 \text{ elsewhere} \quad (3)$$

where Z is the normalization factor:

$$Z = \int_{r_{min}}^{r_{max}} \exp\left[-\frac{1}{2}\left(\frac{r - R_{av}}{\sigma}\right)^2\right] dr \quad (4)$$

In this expression, R_{av} and σ are the average distance and standard deviation of the untruncated Gaussian function, respectively. The standard deviation is related to the half-width of the distribution (hw, full width at half-maximum height) by

$$hw = 2.35\sigma \quad (5)$$

The intensity decay of the donors in the presence of acceptors is therefore described by

$$I_{DA}(t) = I_{DA}{}^0 \int_{r_{min}}^{r_{max}} P(r) \sum_i \alpha_{D_i} \exp\left[-\frac{t}{\tau_{D_i}} - \frac{t}{\tau_{D_i}}\left(\frac{R_0}{r}\right)^6\right] dr \quad (6)$$

where I_{DA} is the emission intensity of the donors at $t = 0$. If the density decrease is only due to the energy transfer, then $I_{DA}{}^0 = I_D{}^0$. $\sum_i \alpha_{D_i}$ is normalized to unity.

In frequency-domain fluorometry, the measured frequency-dependent parameters are the phase shift (ϕ_ω) and modulation (m_ω). The calculated phase shift and modulation are $\phi_{c\omega}$ and $m_{c\omega}$, respectively. They can be calculated from the sine (N_ω) and cosine (D_ω) transforms of the intensity decay function:

$$\phi_{c\omega} = \arctan\left(\frac{N_\omega}{D_\omega}\right) \quad (7)$$

and

$$m_{c\omega} = (N_\omega{}^2 + D_\omega{}^2)^{1/2} \quad (8)$$

$$N_{\omega DA} = \frac{1}{J_{DA}} \int_{r_{min}}^{r_{max}} P(r) \sum_i \frac{\alpha_{D_i} \omega \tau_{DA_i}{}^2}{1 + \omega^2 \tau_{DA_i}{}^2} dr \quad (9)$$

$$D_{\omega DA} = \frac{1}{J_{DA}} \int_{r_{min}}^{r_{max}} P(r) \sum_i \frac{\alpha_{D_i} \tau_{DA_i}}{1 + \omega^2 \tau_{DA_i}{}^2} \quad (10)$$

$$J_{DA} = \int_{r_{min}}^{r_{max}} P(r) \sum_i \alpha_{D_i} \tau_{DA_i} dr \quad (11)$$

The decay times are related to the donor−acceptor distance and the donor-alone decay times by

$$\frac{1}{\tau_{DA_i}} = \frac{1}{\tau_{D_i}} + \frac{1}{\tau_{D_i}}\left(\frac{R_0}{r}\right)^6 \quad (12)$$

The distance distribution parameters (R_{av} and hw) are determined from the calculated phase shift and modulation values by using a nonlinear least-squares fitting procedure. The goodness of fit is characterized by

$$\chi_R{}^2 = \frac{1}{\nu}\sum_\omega \left(\frac{\phi_\omega - \phi_{c\omega}}{\delta\phi}\right)^2 + \frac{1}{\nu}\sum_\omega \left(\frac{m_\omega - m_{c\omega}}{\delta m}\right)^2 \quad (13)$$

where ν is the number of degrees of freedom and $\delta\phi$ and δm are the experimental uncertainties in the measured phase shift and modulation values, respectively.

Correction for Incomplete Acceptor Labeling. The above data analysis will not be effective when donor-labeled molecules lack an acceptor. This is because the donor-alone emission component has kinetics different than those of the donor−acceptor pairs. Moreover, the donor-alone emission contributes to the observed fluorescence in excess of their molar proportion because of the higher quantum yield of the donor in the absence of an acceptor. One must correct for

the incomplete labeling when determining the distance distribution (*32*).

The observed intensity $I(t)$ of the mixture of the donor-alone and donor−acceptor pairs is given by

$$I(t) = I_D{}^m(t) + I_{DA}{}^m(t) \quad (14)$$

where m indicates the decays that are observed from the mixture. Assuming at time = 0 the intensities are unaffected by energy transfer, one has

$$I_D{}^{0m} = (1 - L)I^0 \quad (15)$$

$$I_{DA}{}^{0m} = LI^0 \quad (16)$$

where L denotes the fraction of acceptor labeling and $I^0 = I(t = 0)$ in the presence or absence of acceptor. Combining eqs 1, 6, and 14−16, we obtain eq 17

$$I(t) = I^0(1 - L)\sum_i \alpha_{D_i} \exp(-t/\tau_{D_i}) + LI^0 \int_{r_{min}}^{r_{max}} P(r)\sum_i \alpha_{D_i} \exp\left[-\frac{t}{\tau_{D_i}} - \frac{t}{\tau_{D_i}}\left(\frac{R_0}{r}\right)^6\right] dr \quad (17)$$

The frequency-domain expressions are

$$N_\omega = \frac{1}{J}[(1 - L)J_D N_{\omega D} + LJ_{DA}N_{\omega DA}] \quad (18)$$

$$D_\omega = \frac{1}{J}[(1 - L)J_D D_{\omega D} + LJ_{DA}D_{\omega DA}] \quad (19)$$

$$J = (1 - L)J_D + LJ_{DA} \quad (20)$$

where $N_{\omega DA}$, $D_{\omega DA}$, and J_{DA} are given by eqs 9−11. Thus,

$$N_{\omega D} = \frac{1}{J_D}\sum_i \frac{\alpha_{D_i}\omega\tau_{D_i}{}^2}{1 + \omega^2\tau_{D_i}{}^2} \quad (21)$$

$$D_{\omega D} = \frac{1}{J_D}\sum_i \frac{\alpha_{D_i}\tau_{D_i}}{1 + \omega^2\tau_{D_i}{}^2} \quad (22)$$

$$J_{DA} = \sum_i \alpha_{D_i}\tau_{D_i} \quad (23)$$

In the analysis of the frequency domain data for a system of incomplete acceptor labeling, the determined variables are L, R_{av}, and hw.

RESULTS

Fluorescent Ligands for the Colchicine, Paclitaxel, and GTP Binding Sites on Tubulin. Fluorescent ligands with appropriate spectral and tubulin binding characteristics chosen for the FRET studies are shown in Figure 1. The fluorescence and microtubule-binding properties of the paclitaxel derivative 2-AB-PT have been extensively characterized in our lab (*22*). This ligand was chosen as the energy transfer donor for the colchicine and exchangeable GTP sites. Acceptor ligands for energy transfer from the paclitaxel to the colchicine sites were thiocolchicine and MDL 27048. Both ligands are well characterized in terms of their tubulin-binding and spectroscopic properties (*28*, *29*, *33*). TNP-GTP, which is commercially available, was chosen for the GTP site after determining that the analogue binds to the exchangeable GTP site and supports paclitaxel-induced tubulin assembly (vide infra). Finally, the well-characterized colchicine derivative allocolchicine (*23*) was used as an energy transfer donor for TNP-GTP.

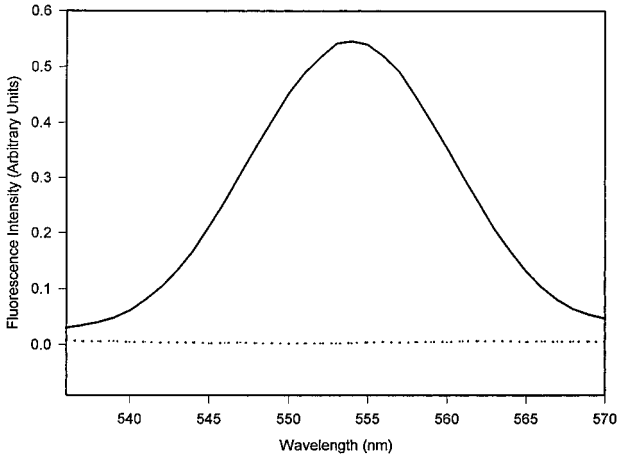

FIGURE 2: Fluorescence emission spectra of tubulin−TNP-GTP in the absence (solid curve) and presence of 1 mM GTP (dotted curve) in PME2 buffer. The preparation of the complexes and the measurement of absorption and emission spectra are described in Experimental Procedures. The concentrations of tubulin and TNP-GTP were 5 and 8.5 μM, respectively. The emission spectrum was recorded at 20 °C, and the excitation wavelength was 410 nm.

Characterization of Tubulin−TNP-GTP. TNP-GTP Binds to the Exchangeable GTP Site on Tubulin. Tubulin−TNP-GTP was prepared from tubulin−GDP as described in Experimental Procedures. HPLC analysis of tubulin−GDP showed that it contained 1 mol of GDP and 1 mol of GTP per mole of tubulin dimer. TNP-GTP binding to tubulin−GDP was observed by fluorescence spectroscopy (Figure 2). Tubulin binding caused a large increase in the intensity of the emission spectrum of TNP-GTP. This increase in fluorescence intensity disappeared completely when excess GTP was added, indicating that TNP-GTP binds to the E-site on tubulin.

Characterization of Tubulin Assembly Induced by TNP-GTP. Assembly of TNP-GTP−tubulin was first performed with a fresh tubulin−TNP-GTP sample prepared as described in Experimental Procedures. It was determined that 0.75 mol of TNP-GTP was bound per mole of tubulin in this sample. The critical concentration for tubulin−TNP-GTP assembly in PME2 buffer in the presence of 20 μM paclitaxel was 0.92 ± 0.03 μM. The critical concentration for tubulin assembly in PMEG buffer under the same experimental conditions was 0.3 ± 0.1 μM. Thus, a 3-fold increase in the critical concentration for tubulin assembly was found with tubulin−TNP-GTP. Electron micrographs of tubulin−TNP-GTP polymerized by paclitaxel showed normal microtubules. Similar results were obtained with the tubulin−TNP-GTP sample previously frozen in liquid nitrogen, indicating the freezing process did not adversely affect the protein properties (data not shown).

Characterization of Protein-Bound FRET Donor−Acceptor Pairs. Paciltaxel and Exchangeable GTP Sites. The emission spectrum of protein-bound 2-AB-PT and the

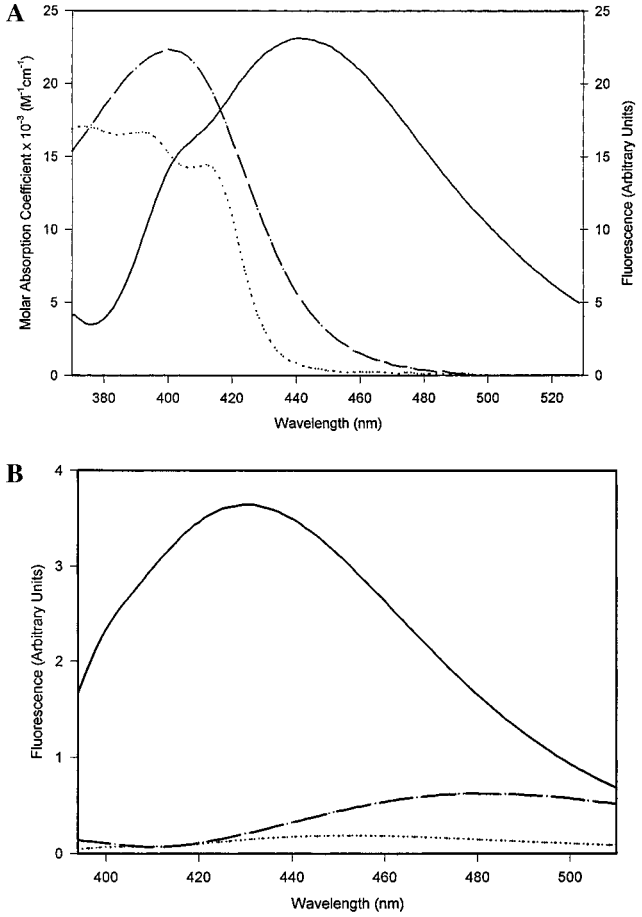

FIGURE 3: (A) Absorption and emission spectra of the donor and acceptor ligands in the colchicine and paclitaxel binding sites: (solid curve) fluorescence emission spectrum of tubulin−2-AB-PT, (dotted curve) absorption spectrum of tubulin−thiocolchicine (dot-dashed curve), and absorption spectrum of tubulin−MDL 27048 complexes. (B) Fluorescence emission spectra of tubulin−2-AB-PT (solid curve), tubulin−2-AB-PT−thiocolchicine (dotted curve), and tubulin−2-AB-PT−MDL 27048 (dot-dashed curve) in PME1 buffer. The concentrations of tubulin and drugs in all solutions were 5 μM. The emission spectrum was recorded at 20 °C, and the excitation wavelength was 320 nm.

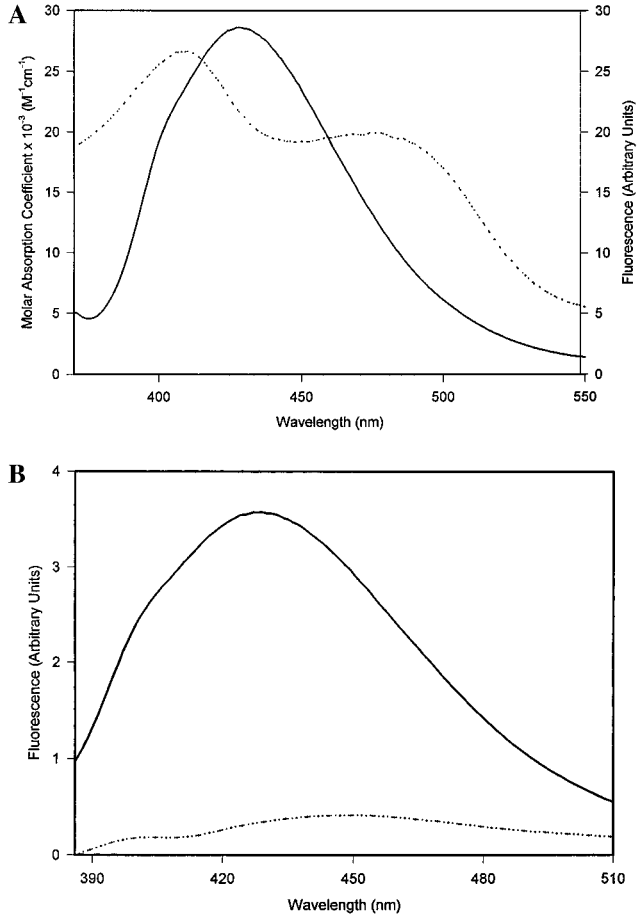

FIGURE 4: (A) Absorption and emission spectra of the donor and acceptor ligands in the paclitaxel and GTP binding sites: (solid curve) fluorescence emission spectrum of tubulin−2-AB-PT and (dotted curve) absorption spectrum of tubulin−TNP-GTP. (B) Fluorescence emission spectra of tubulin−2-AB-PT (solid curve) and tubulin−2-AB-PT−TNP-GTP (dotted curve) in PME2 buffer. The concentrations of tubulin, 2-AB-PT, and TNP-GTP were 5, 2.5, and 8.5 μM, respectively. The emission spectrum was recorded at 20 °C, and the excitation wavelength was 320 nm.

absorption spectrum of protein-bound TNP-GTP are shown in Figure 3A. The spectral overlap integral (J) was calculated to be 6.09×10^{-14} cm^3 M^{-1}, and the Förster distance (R_0) was determined to be 34.5 Å. A decrease in the fluorescence intensity of protein-bound 2-AB-PT was observed in the presence of TNP-GTP, indicating the presence of energy transfer between the donor−acceptor pair (Figure 3B).

2-AB-PT assembled the tubulin−TNP-GTP complex into polymeric structures consisting primarily of normal microtubules, but containing also sheets and protofilaments (data not shown).

Colchicine and Paclitaxel Sites. Figure 4A shows the emission spectrum of microtubule-bound 2-AB-PT (donor) and the absorption spectra of tubulin-bound thiocolchicine and tubulin-bound MDL 27048 (acceptor ligands). The spectral overlap integral (J) was calculated to be 2.96×10^{-14} cm^3 M^{-1} for the donor−acceptor pair 2-AB-PT−thiocolchicine and 3.41×10^{-14} cm^3 M^{-1} for 2-AB-PT−MDL 27048. Accordingly, Forster distances (R_0) were determined to be 30.6 and 31.4 Å, respectively.

Paclitaxel and 2-AB-PT induce tubulin to assemble into normal microtubules (*22*, *34*). When tubulin is in the form of the colchicine−tubulin complex, however, nonmicrotubule polymers such as sheets of protofilaments and amorphous aggregates result (*12*, *35*). It was therefore important to examine the structure of the polymeric species formed when tubulin bound to thiocolchicine (tubulin−thiocolchicine) and tubulin bound to MDL 27048 (tubulin−MDL 27048) were assembled by 2-AB-PT. Electron micrographs of the polymers formed by 2-AB-PT with tubulin−thiocolchicine and tubulin−MDL 27048 showed polymer sheets in both systems.

Fluorescence emission spectra of tubulin−2-AB-PT (donor-only), tubulin−2-AB-PT−thiocolchicine (donor−acceptor), and tubulin−2-AB-PT−MDL 27048 (donor−acceptor) are shown in Figure 4B. A decrease in the fluorescence emission intensity of tubulin-bound 2-AB-PT was observed in the presence of each acceptor ligand. These spectra indicate that fluorescence energy transfer between the donor and acceptor ligands occurs in both systems.

Colchicine−Exchangeable GTP Sties. The binding of allocolchicine to the colchicine site on tubulin is accompanied by a large increase in the emission intensity of allocolchicine

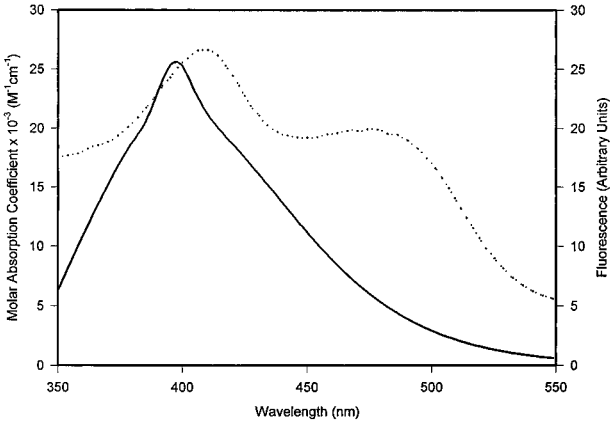

FIGURE 5: Absorption and emission spectra of the donor and acceptor ligands in the colchicine and GTP binding sites in PME2 buffer: (solid curve) fluorescence emission spectrum of allocolchicine bound to tubulin and (dotted curve) absorption spectrum of TNP-GTP bound to tubulin. The concentrations of tubulin, allocolchicine, and TNP-GTP were 5, 5, and 8.5 μM, respectively. The emission spectrum was recorded at 20 °C, and the excitation wavelength was 320 nm.

(*23*). The emission spectrum of tubulin-bound allocolchicine possesses sufficient overlap with the absorption spectrum of TNP-GTP for FRET to occur (Figure 5). The spectral overlap was calculated to be 4.76×10^{-14} cm^3 M^{-1} and the Förster distance (R_0) was determined to be 37.0 Å. However, no energy transfer was observed between this donor−acceptor pair in either the steady-state spectra or the time-resolved data.

Determination of Distances between the Colchicine, Paclitaxel, and Exchangeable GTP Binding Sites Using FRET. An accurate determination of the distance between fluorophores using FRET requires careful consideration of experimental conditions. For example, the sample solutions must be prepared such that changes in emission parameters in the presence of an acceptor can be reliably ascribed to resonance energy transfer. A decrease in donor emission intensity accompanied by an increase in acceptor emission intensity may be due to a radiative process (e.g., observed donor emission intensity decreased due to the absorption of a photon by acceptor), which is not subject to Förster theory (*19*). Radiative energy transfer does not affect the lifetime of the donor, which was the parameter used to quantitatively evaluate FRET in this work. High concentrations of the acceptor may decrease the observed signal intensity from the donor; thus, low concentrations of acceptor ligands were employed in the time-resolved measurements. Steady-state spectra, which will be affected by radiative energy transfer and other optical properties of the sample, are shown to illustrate the presence of FRET in our systems, but were not employed in quantitative analysis.

A consequence of low acceptor concentrations in the FRET experiment may be incomplete acceptor labeling. The distance distribution between donors and acceptors is recovered from the intensity decay kinetics of the donor in the presence and absence of the acceptor (*30, 32*). If donor fluorophores lack an acceptor in the donor−acceptor complex, the emission data of the complex will also contain the donor-alone component. For example, the fraction of acceptor labeling under these experimental conditions was determined to be 0.91 for 2-AB-PT−thiocolchicine and 0.88 for 2-AB-PT−MDL 27048. Correction for incomplete acceptor labeling for frequency domain data was therefore performed as described in Experimental Procedures.

Table 1: Distance Distribution of the Donor−Acceptor Pairs[a]

donor−acceptor pair	R_0 (Å)	R_{av} (Å)	hw (Å)
2-AB-PT−thiocolchicine	30.6	17.5	3.0
2-AB-PT−MDL 27048	31.4	17.3	0.8
2-AB-PT−TNP-GTP	34.5	16.0	17.9
allocolchicine−TNP-GTP	37.0	nd	nd

[a] R_0 is the distance between the donor and acceptor when the FRET efficiency = 50%. R_{av} is the average distance between the donor and acceptor. hw is the half-width of distance distribution. nd is not detected.

Colchicine−Paclitaxel Sites. The distance distribution between the colchicine and paclitaxel sites on the polymer was calculated from the decay kinetics of the protein-bound 2-AB-PT as described in Experimental Procedures. An average distance of 17.4 Å between the paclitaxel and colchicine sites was found with each donor−acceptor pair (Table 1). Furthermore, the half-width of the distance distribution was narrow (≤3 Å), indicating that a single distance was being measured.

Exchangeable GTP−Paclitaxel Site. The distance distribution was determined between the GTP E-site and paclitaxel site on tubulin polymers, as we have been unable to discover experimental conditions under which these experiments could be performed on the unassembled tubulin dimer. An average distance of 16.0 Å between the sites was determined, but the half-width of the distance distribution was 17.9 Å (see Table 1). A large half-width for the distance distribution indicates that FRET occurs between more than one donor−acceptor pair (*30*).

DISCUSSION

Measurement of FRET is a powerful and valuable technique for determining distances between fluorophores (*18, 19*). Tubulin is a good protein for this type of analysis, as it is relatively small and possesses a reasonable number of binding sites for endogenous and exogenous ligands that could be exploited for fluorescence energy transfer measurements. In this work, FRET was successfully used to determine the distance between two important drug binding sites on tubulin: the colchicine site and the paclitaxel site.

Although FRET measurements for the colchicine−paclitaxel sites were performed on tubulin sheets rather than on the tubulin heterodimer, we believe that an intrasubunit distance is being observed. Our finding of a 17 Å distance between the colchicine binding site and the C-2 region of the paclitaxel binding site fits well into the current knowledge of the colchicine and paclitaxel binding sites. The paclitaxel binding site on zinc-induced tubulin sheets has been observed at the interprotofilament contact region by electron microscopy and assigned to the β-subunit from photoaffinity labeling (*36*−*38*). On the basis of photoaffinity labeling and thermodynamic studies, the colchicine site is proposed to be on β-tubulin, close to the $\alpha\beta$-subunit interface (*40*−*43*). The current model of tubulin structure easily accommodates our result of a 17 Å distance between colchicine and paclitaxel sites.

The FRET data obtained did not provide a single distance for the paclitaxel−GTP sites. These data are, however,

significant. First, the utility of time-resolved measurements is dramatically illustrated. Had calculations been performed using steady state data, a single distance between the two sites could have been obtained, which would have been in error. Simultaneous determination of the distribution of the distances revealed that energy transfer between more than one donor−acceptor pair was occurring in the sample.

Although we were unable to resolve the distances between multiple donor−acceptor pairs, the existence of more than one FRET process in the sample provides an indication of the relationship between the paclitaxel and exchangeable GTP binding sites on the microtubule. Electron micrographs of the polymers bound with the fluorescent probes showed a preponderance of microtubules, implying that the signal heterogeneity was not artifactual. Thus, the exchangeable GTP binding sites within the polymer could be arranged in such a way that two or more acceptors experience energy transfer from a single donor fluorophore. Since the R_0 for the donor−acceptor pair for these sites is quite large (34.5 Å), acceptors up to 50 Å away from the donor could conceivably influence the decay kinetics of the donor. The axial dimensions of a heterodimer subunit are 35−40 and 50−55 Å. One interpretation of the FRET data, then, is that the paclitaxel fluorophore serves as an energy transfer donor to two GTP site acceptors: one within the same subunit and one on an adjacent protofilament.

We were initially very surprised that we observed no energy transfer between the colchicine and exchangeable GTP sites in our samples. Previously, Ward and Timasheff (*21*) observed no energy transfer using allocolchicine and Co^{2+} as the donor−acceptor pair for the colchicine site and GTP E-site, respectively. On the basis of an R_0 value of 14.7 Å for this donor−acceptor pair, they estimated that the colchicine site and GTP E-site on tubulin were separated by at least 24 Å. We had hoped that the allocolchicine−TNP-GTP pair, with an R_0 value of 37.0 Å, would be able to exhibit FRET between the two sites. We were unable to take full advantage of the increased observation range for this pair, however, due to the decreased affinity of TNP-GTP for tubulin. Assuming that an energy transfer efficiency of 10% or less could not be detected in the system and accounting for the incomplete binding of TNP-GTP, we estimate that the colchicine and exchangeable GTP binding sites are at least 40 Å apart. Clearly, colchicine binding to tubulin gives rise to long range conformational changes in the protein.

Possible Spatial Relationships between the Paclitaxel, Colchicine, and GTP Binding Sites on Tubulin and Microtubules. Figure 6 shows a diagram of one possible arrangement of the three binding sites on tubulin and the microtubule. All three binding sites are placed on β-tubulin in accordance with photoaffinity labeling and other results (see, for example, refs *38* and *41*−*44*). The paclitaxel site is located near the interprotofilament contact region (*36*), and the colchicine binding site is believed to be near the intradimer contact region. The GTP binding site is placed at the average distance obtained from FRET (16 Å), near the longitudinal dimer contact region and far from the colchicine binding site.

We have recently had the opportunity to examine an atomic model of the tubulin dimer obtained by electron crystallography of zinc-induced tubulin sheets in which the paclitaxel and GTP sites are discernible (*45*). Our interpretation of the paclitaxel−GTP site FRET data is consistent with the structural features observed in the tubulin sheets. The colchicine binding site is not seen in the structure since it is unoccupied in the sample, but an amino acid identified by affinity labeling as being involved in the colchicine binding site (C356; *43*) is found at the interface of the two subunits at a distance from the paclitaxel site that is well within the distance we determined from FRET analysis.

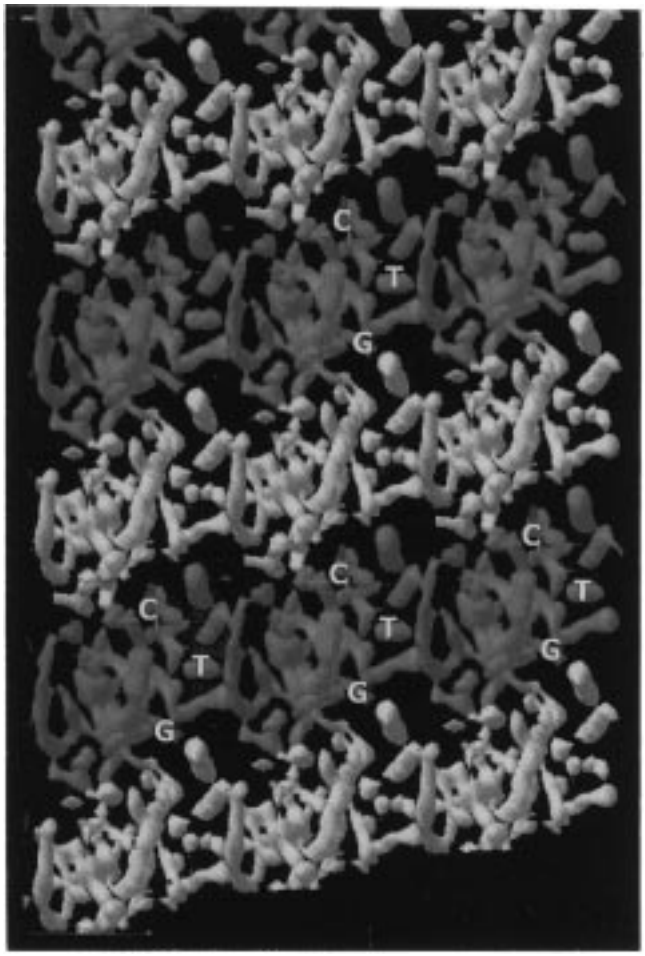

FIGURE 6: Possible relative locations of the colchicine (C), paclitaxel (T), and exchangeable GTP (G) binding sites on tubulin. The protofilament images were obtained from electron crystallography data (*16*) and were provided by K. Downing. Identical images of a single protofilament were selected and were aligned according to Song and Mandelkow (*46*, *47*).

ACKNOWLEDGMENT

We are indebted to Dr. Vincent Peyrot for the gift of MDL 27048 and to Dr. Barbara M. Poliks for performing the electron microscopy. We thank Dr. James L. Potenziano, Jr., for synthesizing allocolchicine. We are grateful to Dr. K. Downing for providing the protofilament image and for his assistance in aligning the protofilaments in the illustration and to Dr. Eva Nogales for allowing us to examine her tubulin structure prior to its publication.

REFERENCES

1. Dustin, P. (1984) *Microtubules*, 2nd ed., Springer-Verlag, New York.
2. Engelborghs, Y. (1990) in *Microtubule Proteins* (Avila, J., Ed.) Boca pp 1−88, CRC Press, Boca Raton, FL.

3. Unger, E., Bohm, K. J., and Vater, W. (1986) *Acta Histochem. 33*, 85−94.
4. Polin, L., Valeriote, F., White, K., Panchapor, C., Pugh, S., Knight, J., LoRusso, P., Hussain, M., Liversidge, E., Peltier, N., Golakoti, T., Patterson, G., Moore, R., and Corbett, T. H. (1997) *Invest. New Drugs 15*, 99−108.
5. Goldspiel, B. R. (1997) *Pharmacotherapy 5*, 110S−125S.
6. Hudes, G. (1997) *Semin. Urol. Oncol. 15*, 13−19.
7. Hamel, E. (1990) in *Microtubule Proteins* (Avila, J., Ed.) pp 89−191, CRC Press, Boca Raton, FL.
8. Hastie, S. B. (1991) *Pharmacol. Ther. 51*, 377−401.
9. Schiff, P., and Horwitz, S. B. (1980) *Proc. Natl. Acad. Sci. U.S.A. 77*, 1561−1565.
10. Bollag, D., McQueney, P. A., Zhu, J., Hensens, O., Koupal, L., Liesch, J., Goetz, M., Lazarides, E., and Woods, C. (1995) *Cancer Res. 55*, 2325−2333.
11. Himes, R. H. (1991) *Pharmacol. Ther. 52*, 257−267.
12. Howard, W. D., and Timasheff, S. N. (1988) *J. Biol. Chem. 263*, 1342−1346.
13. Correia, J. J. (1991) *Pharmacol. Ther. 52*, 127−147.
14. Carlier, M., and Pantaloni, D. (1983) *Biochemistry 22*, 4814−4822.
15. Arnal, I., and Wade, R. H. (1995) *Curr. Biol. 5*, 900−908.
16. Wolf, S. G., Nogales, E., Kikkawa, M., Gratzinger, D., Hirokawa, N., and Downing, K. H. (1996) *J. Mol. Biol. 262*, 485−501.
17. Bayley, H. (1983) *Laboratory Techniques in Biochemistry and Molecular Biology: Photogenerated Reagents in Biochemistry and Molecular Biology*, Vol. 12, Elsevier, New York.
18. Stryer, L. (1978) *Annu. Rev. Biochem. 47*, 819−846.
19. Lackowicz, J. R. (1983) *Principles of Fluorescence Spectroscopy*; Plenum Press, New York.
20. Ward, L. D., Seckler, R., and Timasheff, S. N. (1994) *Biochemistry 33*, 11900−11908.
21. Ward, L. D., and Timasheff, S. N. (1988) *Biochemistry 27*, 1508−1514.
22. Han, Y., Chaudhary, A. G., Chordia, M. D., Perez-Ramirez, B., Kingston, D. G. I., and Bane, S. (1996) *Biochemistry 35*, 14173−14183.
23. Hastie, S. B. (1989) *Biochemistry 28*, 7753−7760.
24. Hahn, K., Humpreys, W. G., Helm, A. M., Hastie, S. B., and Macdonald, T. L. (1991) *Bioorg. Med. Chem. Lett. 1*, 471−476.
25. Williams, R. C., Jr., and Lee, J. C. (1982) *Methods Enzymol. 85*, 376−385.
26. Penefsky, H. A. (1977) *J. Biol. Chem. 252*, 2891−2899.
27. Dietrich, H. W., III, and Williams, R. C., Jr. (1978) *Biochemistry 17*, 3900−3907.
28. Chabin, R., Feliciano, F., and Hastie, S. B. (1990) *Biochemistry 29*, 1869−1875.
29. Peyrot, V., Leynadier, D., Sarrazin, M., Briand, C., Rodriguez, A., Nieto, J. M., and Andreu, J. M. (1989) *J. Biol. Chem. 264*, 21296−21301.
30. Lakowicz, J. R., Gryczynski, I., Laczko, G., and Joshi, N. (1991) in *Luminescence Techniques in Chemical and Biochemical Analysis* (Baeyens, W. R. G., Keukeleire, D. De., and Korkidis, K., Eds.) pp 141−177, Marcel Dekker, Inc., New York.
31. Seckler, R., Wu, G., and Timasheff, S. N. (1990) *J. Biol. Chem. 265*, 7655−7661.
32. Lackowicz, J. R., Gryczynski, I., Wiczk, W., Kusba, J., and Johnson, M. L. (1991) *Anal. Biochem. 195*, 243−254.
33. Peyrot, V., Leynadier, D., Sarrazin, M., Briand, C., Menendez, M., Laynez, J., and Andreu, J. M. (1992) *Biochemistry 31*, 11125−11132.
34. Parness, J., and Horwitz, S. B. (1981) *J. Cell Biol. 2*, 479−487.
35. Andreu, J. M., Wagenknecht, T., and Timasheff, S. N. (1983) *Biochemistry 22*, 1556−1566.
36. Nogales, E., Wolf, S. G., Khan, I. A., Luduena, R. F., and Downing, K. H. (1995) *Nature 375*, 424−427.
37. Rao, S., Krauss, N. E., Heerding, J. M., Swindell, C. S., Ringel, I., Orr, G. A., and Horwitz, S. B. (1994) *J. Biol. Chem. 269*, 3132−3134.
38. Rao, S., Chaudhary, A. G., Kingston, D. G. I., and Horwitz, S. B. (1995) *J. Biol. Chem. 270*, 20235−20238.
39. Williams, R. F., Mumford, C. L., Williams, G. A., Floyd, L. J., Aivaliotis, M. J., Martinez, R. A., Robinson, A. K., and Barnes, L. D. (1985) *J. Biol. Chem. 260*, 13794−13802.
40. Floyd, L. J., Barnes, L. D., and Williams, R. F. (1989) *Biochemistry 28*, 8515−8525.
41. Wolff, J., Knipling, L., Cahnmann, H. J., and Palumbo, G. (1991) *Proc. Natl. Acad. Sci. U.S.A. 88*, 2820−2824.
42. Shearwin, K. E., and Timasheff, S. N. (1994) *Biochemistry 33*, 894−901.
43. Bai, R., Pei, X., Boye, O., Gettahun, Z., Grover, S., Nguyen, N. Y., Brossi, A., and Hamel, E. (1996) *J. Biol. Chem. 271*, 12639−12645.
44. Shivanna, B. D., Mejillano, M. R., Williams, G. A., and Himes, R. A. (1993) *J. Biol. Chem. 268*, 127−132.
45. Nogales, N., Wolf, S. G., and Downing, K. H. (1998) *Nature 391*, 199−203.
46. Song, Y.-H., and Mandelkow, E. (1993) *Proc. Natl. Acad. Sci. U.S.A. 90*, 1671−1675.
47. Song, Y.-H., and Mandelkow, E. (1995) *J. Cell Biol. 128*, 81−94.

BI9719760